ELSEVIER

Journal of Molecular Catalysis A: Chemical 191 (2003) 101–112

JOURNAL OF MOLECULAR CATALYSIS A: CHEMICAL

www.elsevier.com/locate/molcata

A parametrical embedding method for catalytic modeling

Flor Marina Poveda [a], Javier Fernandez-Sanz [b], Fernando Ruette [c,*]

[a] *Grupo de Química Teórica, Universidad Nacional de Colombia, Bogota, Colombia*
[b] *Departamento de Química Fisica, Universidad de Sevilla, E-41012, Sevilla, Spain*
[c] *Laboratorio de Química Computacional, Centro de Química, IVIC, Caracas, Venezuela*

Received 1 February 2002; accepted 20 June 2002

Abstract

In this work, an embedding procedure is proposed for parametric methods. An application to modeling a nickel catalyst supported on γ-alumina was carried out by considering a set of point charges and parametric functionals to simulate short- and long-range interactions. Several clusters were calculated Al_nO_m and $Al_nO_mNi_o$ ($n = 4, 8, 14, 18, 20$; $m = 6, 12, 21, 27, 30$; $o = 1$–5). An analysis of calculated properties for different cluster sizes indicates that, in order to model chemical properties in an adequate way, a minimum cluster size is required. Results show that the long-range effects in the modeling of Ni cluster formation on alumina have to be considered, because they produce changes in bond energies and charges.

Keywords: Embedding; Alumina; Nickel cluster; Parametric method

1. Introduction

Modeling the whole process of a catalytic reaction implies the study of several steps, such as, physisorption, chemisorption, diffusion, surface reaction, and desorption in which for each one coverage effects play an important role. Therefore, a fair representation of a catalytic system often leads to a model that is usually intractable for standard ab initio quantum chemistry methods. A typical example corresponds to a catalyst formed by the dispersion of relatively small metallic clusters on a support. In many cases, the cluster-support interactions are relevant for the modeling of the adsorption site. Hence, a more realistic modeling of the catalyst, other than a few atoms cluster, has to be considered. Thus, a reasonable catalyst cluster model has to include several adsorption sites plus a support aggregate of sufficient size to mimic correctly the catalyst- and adsorbate-support interactions. The support model size may be also an important issue in order to evaluate activation barrier heights and the stability of intermediates. In some cases, surface transient species are strongly affected by the support, specially, if both have ionic nature. Thus, the electric field generated by the environment of an active site may be of great significance in the kinetics and reactivity of the catalytic system (long-range effects).

The above mentioned systems are convenient examples for the use of embedding techniques. A suitable model of a catalyst site on an ionic support may be a cluster embedded into a very large aggregate of support atoms represented by point charges. As said above, the model of the whole catalyst is fundamental, particularly, to study reactions affected by surface processes, such as, coverage, cooperative effects, island formation, addition of promoters, creation of

* Corresponding author.
E-mail address: fruette@ivic.ve (F. Ruette).

1381-1169/02/$ – see front matter
PII: S1381-1169(02)00355-2

vacancies, induced surface roughness, sintering of dispersed particles, etc.

The basic idea of embedding approach come from dividing a large system, at least, in two different regions. One represents the local region where modeled processes occur and other, the largest region (environment) in which the former region is embedded. Usually, model potentials are adopted to represent the interaction between the local region and the surrounding environment.

Embedding techniques have been employed in the last decade in many fields using different type of methods. Early embedding approaches based on local space approximation (LSA) [1,2] and embedded atom method (EAB) [3,4] has been applied to transition metals. A pioneer work by Whitten and Pakkanen [5], and Yang and Whitten [6] handled post-Hartree-Fock methods using cluster-within-a-cluster (CC) approach for transition metals. More recently, several approaches of embedded clusters based on model potentials has been proposed by Barandarián and Seijo [7,8] using the ab initio model potential (AIMP) method. Mejías and Fernandez-Sanz presented an ab initio compact model potential (CMP) extended to spin dependent properties [9–11]. Various embedding approaches employing DFT methods have been applied by using localization procedures and fractional occupation orbitals [12], explicit correlation in a periodic potential [13], divided-and-conquer approach [14], self-consistent cluster embedding method [15], moderately large embedded cluster [16], and cluster embedding with lattice polarization that includes a hybrid QM/MM approach [17–19].

Different embedding procedures have been developed using Green-function approaches by Pisani et al. [20,21] and more recently by Inglesfield and coworkers [22] using function matching. Several embedding techniques based on ab initio methods, such as, central-cluster approach for crystalline solids [23], shell-model representation [24], a CC approach with a novel localization procedure [25], and point charge cluster (PCC) with charge density consistence [26] have been reported.

The size of the embedded cluster is very relevant, as mentioned above, in modeling several steps in catalytic reactions. One of the advantages of parametric methods (methods based on parameters, such as, semiempirical ones) is their capability to calculate, in a reasonable time, a very large cluster that includes several adsorbates and various types of adsorption sites, indispensable for multi-functional reactions. Embedding methods has been already applied at semi-empirical level [27] for large clusters using SINDO1 method [28]. Normally, transition metal systems imply open-shell calculations that require searching for different states associated to different spins and electronic configurations. Quantum parametric methods allow the possibility of exploring electronic properties of very heavy and complex systems.

The aim of this work is to propose and test an embedded cluster method based on a parametric Hamiltonian. In this approach, the interaction cluster-environment is modeled through parametric functionals, similar to those employed in parametric methods. The selected example corresponds to the growing of Ni catalyst supported on an alumina cluster embedded into a very large cluster of charges. The paper is organized as follows. In Section 2, theoretical foundations and the employed methodology are presented. In Section 3, parameters for the parametric and embedding methods are described. In addition, variation of atomic charges and diatomic binding energies (DBEs) for several alumina clusters, and the effect of embedding in alumina–Ni clusters are analyzed. Finally a summary of the most important features found in this work is presented in Section 4.

2. Theoretical foundations and methodology

A model Hamiltonian (H_{mH}) for a system A embedded into a large system BC (see schematic representation in Fig. 1) can be defined according to [29,30] as

$$H_{\mathrm{mH}}^{\mathrm{A}} = H_{\mathrm{o}}^{\mathrm{A}} + W_{\mathrm{mH}}^{\mathrm{A-BC}} \tag{1}$$

where

$$H_{\mathrm{o}}^{\mathrm{A}} = \sum_{i\in\mathrm{A}} \left(-\nabla_i^2 + \sum_{\alpha\in\mathrm{A}} \left(\frac{Z_\alpha}{R_{\alpha i}} \right) + \sum_{j\in\mathrm{A}} V_{ij} \right) \tag{2}$$

The term $W_{\mathrm{mH}}^{\mathrm{A-BC}}$ corresponds to the intersubsystem interaction operator between system A (a cluster) and the BC environment. It can be divided in two terms: electronic and nuclear

$$W_{\mathrm{mH}}^{\mathrm{A-BC}} = W_{\mathrm{mHe}}^{\mathrm{A-BC}} + W_{\mathrm{mHn}}^{\mathrm{A-BC}} \tag{3}$$

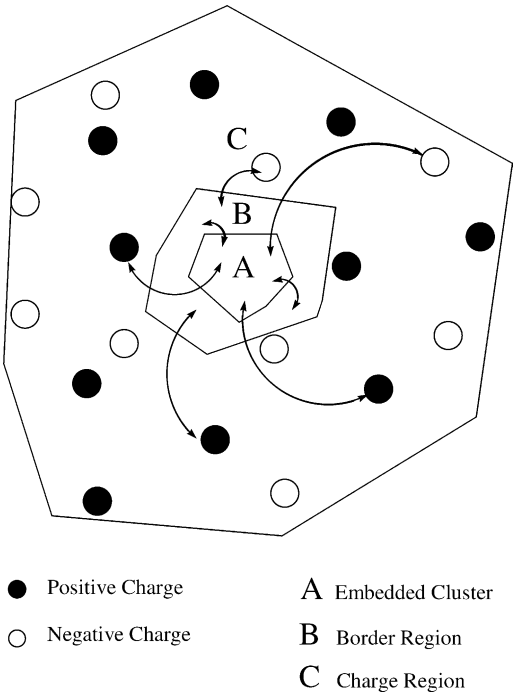

Fig. 1. Scheme of embedding interactions and regions.

where

$$W_{\mathrm{mHe}}^{\mathrm{A-BC}} = J^{\mathrm{BC}} - K^{\mathrm{BC}} + V^{\mathrm{BC}} + P^{\mathrm{BC}} \tag{4}$$

The terms J^{BC}, K^{BC}, and V^{BC} correspond to Coulomb, exchange, and attractive potential of electrons on A with atoms on B and C regions, respectively. P^{BC} is a projection operator that intended to represent the cluster-environment orthogonality condition.

$$P^{\mathrm{BC}} = \sum_i |\phi_i^{\mathrm{BC}}\rangle(\varepsilon_i^{\mathrm{BC}})\langle\phi_i^{\mathrm{BC}}| \tag{5}$$

where ϕ_i^{BC} are spin orbitals defined in the B and C regions.

A suitable scheme to define the $W_{\mathrm{mHe}}^{\mathrm{A-BC}}$ operator was proposed by Mejías and Fernandez-Sanz [9] as divided into short- ($W_{\mathrm{mHe}}^{\mathrm{sr}}$) and long-range ($W_{\mathrm{mHe}}^{\mathrm{lr}}$) terms. These authors express the ($W_{\mathrm{mHe}}^{\mathrm{sr}}$) term in a basis set $\{\varphi\}$ representation as

$$W_{\mathrm{mHe}}^{\mathrm{sr}} = \sum_{\rho\sigma\in\mathrm{B}} |\varphi_\rho > C_{\rho\sigma} < \varphi_\sigma| \tag{6}$$

The set of coefficients $\{C_{\rho\sigma}\}$ is the contribution of Coulomb, exchange and projection operators. The corresponding $(W_{\mathrm{mHe}}^{\mathrm{sr}})_{\mu\mu}$ functional, considering the zero differential overlap (ZDO) approach in parametric Hamiltonians [31], can be expressed as

$$(W_{\mathrm{mHe}}^{\mathrm{sr}})_{\mu\mu} = \omega_{\mathrm{XY}}(I_\mu + I_\rho)S_{\mu\rho}|S_{\mu\rho}| \quad (\mu \in \mathrm{X} \in \mathrm{A};\quad \rho \in \mathrm{Y} \in \mathrm{B}) \tag{7}$$

Here ω_{XY} is an adjustable constant similar to the term used in the parametric resonance integral for the XY pair of atoms (X ∈ A, Y ∈ B). The constants I_μ and I_ρ correspond to ionization potentials for μ and ρ electrons in X and Y, respectively. Notice that this expression is alike to those used for one-electron two-center interaction approximation in most of the parametric methods [32]. The overlap module $|S_{\mu\rho}|$ is included in order to maintain rotational invariance that occurs when the zero differential approach (ZDO) is employed [31]. Notice that the product $|S_{\mu\rho}|S_{\mu\rho}$ decays rapidly with the distance, therefore, expression (7) has a significant value only for A–B interactions. Electrostatic interactions between A and B are considered in expression (7), as mentioned in the $C_{\rho\sigma}$ coefficients in (6). This approach also avoids a strong charge polarization of cluster edge atoms in A.

The long-range term associated to electrostatic inter-atomic electron-nucleus interaction is represented in several parametric methods by considering the neglect penetration integral (NPI) approximation [31], expressed in terms of two-center electron repulsion integrals. This approach has been confirmed to be a good approximation for electronic electrostatic interaction, at relatively long distances [33,34]. Thus, a similar expression to NPI approximation was considered to mimic electron–electron and electron–nucleus long-range electrostatic interactions, in a simple way

$$(W_{\mathrm{mHe}}^{\mathrm{lr}})_{\mu\mu} = -\lambda_{\mathrm{ac}} q_{\mathrm{c}} \gamma_{\mu\rho} \quad (\mu \in \mathrm{A};\quad \rho \in \mathrm{C}) \tag{8}$$

where λ_{ac} is an adjustable parameter for each ac pair of atoms, q_{c} corresponds to the charge on c atom, and $\gamma_{\mu\rho}$ is a electron–electron repulsion integral between an electrons in $\varphi_\mu \in$ A and an electron in $\varphi_\rho \in$ C. These integrals are expressed in terms of one-center integrals ($\gamma_{\mu\mu}$ and $\gamma_{\rho\rho}$), according to the Ohno–Klopman (OK) approximation [35,36]. If atoms in C are neutral, the repulsive electron–electron and the attractive electron–nucleus interactions are counterbalanced at long distances. On the other hand, if atoms in C are positively charged, the net interaction is attractive;

inversely, if c atoms are negatively charged, the interaction is repulsive. Thus, the total electrostatic interaction between an electron in $\varphi_\mu \in$ A with electrons and nucleus of c $\in$ C can be approximated by the interaction of the μ electron with the net atomic charge of q_c.

The long-range interaction of an a core (Z_a charge) with a charged q_c atom (nucleus–electron and nucleus–nucleus) may be evaluated by an expression similar to that of core–core repulsion used in previous works [33,34,37]

$$W_{\mathrm{mHn}}^{\mathrm{A-C}} = Z_a q_c \left(\gamma_{s_a s_c} + \left(\frac{1}{R_{ac} - \gamma_{s_a s_c}} \right) \alpha_{ac} e^{-R_{ac}} \right) \quad (9)$$

where Z_a, α_{ac}, $\gamma_{s_a s_c}$, and R_{ac} are nuclear core charge, an adjustable parameter, average electron–electron repulsion integral or between s orbitals, and inter-nuclear distance between a and c atoms, respectively. Notice that as a c atom in C is positively charged, the net interaction is repulsive; conversely, for a negatively charged c atom, the interaction is attractive.

The quantum method employed here is based on a parametric Hamiltonian (H_{pa}) obtained from simulation techniques. In previous works [33,34,38], optimization of H_{pa} for molecular systems was proposed in terms of binding energies of X–Y bonds from experimental data or results of very well-defined methods. X and Y stand for molecular fragments, as well as, the atoms that form the X–Y bond.

$$\min \left\| H_{exa}^{XY} - H_{pa}^{XY} \right\| = \min \left(\sum_i |\mathrm{BE}_{exa_I}^{XY} - \mathrm{BE}_{pa_I}^{XY}|^2 \right)^{1/2} \quad (10)$$

where

$$\mathrm{BE}^{XY} = \langle \Psi_I^{XY} | H^{XY} | \Psi_I^{XY} \rangle - \langle \Psi^X | H^X \Psi^X \rangle - \langle \Psi^Y | H^Y | \Psi^Y \rangle \quad (11)$$

This formalism has been implemented in a modular code called CATIVIC [39] based on MINDO/SR [37] in which several parametric functionals, new computational tools, and different parametrization methods were included, for studying surface–adsorbate interactions.

Table 1
Aluminum atomic parameters

Parameter	ss	sp	pp
U_{core} (eV)	25.76	–	18.37
F_0 (a.u.)	0.29732	0.24366	0.20556
F_2 (a.u.)	–	–	0.08881
G_1 (a.u.)	–	0.07718	–

3. Results and discussion

Before starting calculations, evaluation of parameters was performed. A procedure based on Eqs. (10) and (11) was used for optimization of atomic parameters (Slater–Condon and core integral) but using excitation energies obtained from Moore's Tables [40]. Because we are interested in study the feasibility of this embedding technique, only new atomic parameters were obtained for those atoms that are unknown, for example, Al atom. The method employed for optimized parameters is based in simulated annealing [41], considering only the energy difference between excited states and the ground state. Parameters for Al are presented in Table 1. Atomic parameters for Ni and O atoms were taken from earlier work [42]. Molecular parameters (β, for resonance integral functional; α, for core–core potential that includes frozen core correction and interatomic correlation [38]) for Al–X (X = O, Al, Ni) and Ni–O were evaluated considering the adjustment with respect to experimental BE and equilibrium bond distances of diatomic molecules [43–46]. Values of these new parameters are displayed in Table 2. Different electronic configurations and states were evaluated to assure that parametrization was carried out with the lowest electronic state.

In order to analyze effect of surrounding atoms on an adsorption site, it is necessary to study electronic property changes of selected atoms as the

Table 2
Molecular parameters

Parameter	Atom pair				
	Al–O	Ni–Ni	Al–Al	Ni–Al	Ni–O
α	0.79881	1.19112	2.57690	2.70800	2.47526
β	0.59301	0.99066	0.36618	1.04325	1.41091

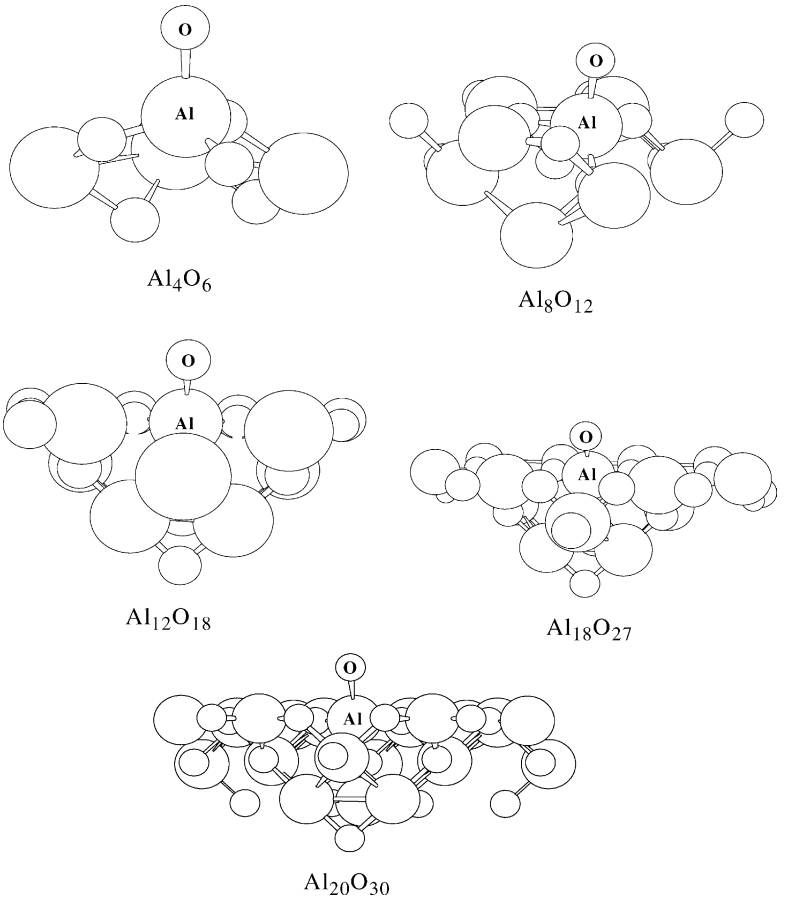

Fig. 2. Alumina clusters.

cluster size increases. Therefore, calculations were carried out for a series of γ-alumina clusters: Al_4O_6, Al_8O_{12}, $Al_{14}O_{21}$, $Al_{18}O_{27}$, and $Al_{20}O_{30}$. The structure of these clusters is presented in Fig. 2. All of them were taken from the (1 1 0) surface structure described elsewhere [11]. Clusters were also selected considering the same stoichiometry than Al_2O_3 and, of course, charge equal to zero. The adsorption site considered corresponds to an oxygen atom in a tetrahedral environment, see atom O(5) in clusters and Al(1) in clusters of Fig. 2. This site was chosen to study the nickel adsorption, because theoretical [47–49] and experimental [50] researches both indicate that tetrahedral Al sites are the most active site in γ-Al_2O_3. The strategy followed in this work is to understand what happens with site properties, as the cluster size increases, and then to use the most adequate cluster (that converges in the site properties) to be embedded into a large set of charges, as shown in Fig. 3.

Results of variation of charge density on O(5) and equilibrium bond distance Al(1)–O(5) with the

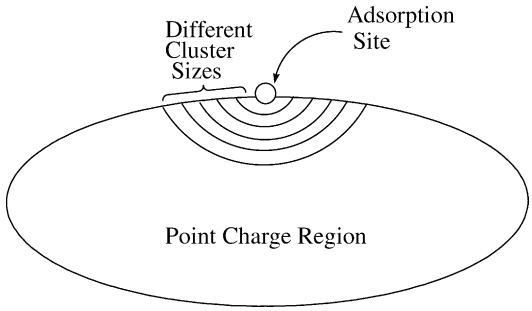

Fig. 3. Scheme of selected clusters embedded on a set of point charges.

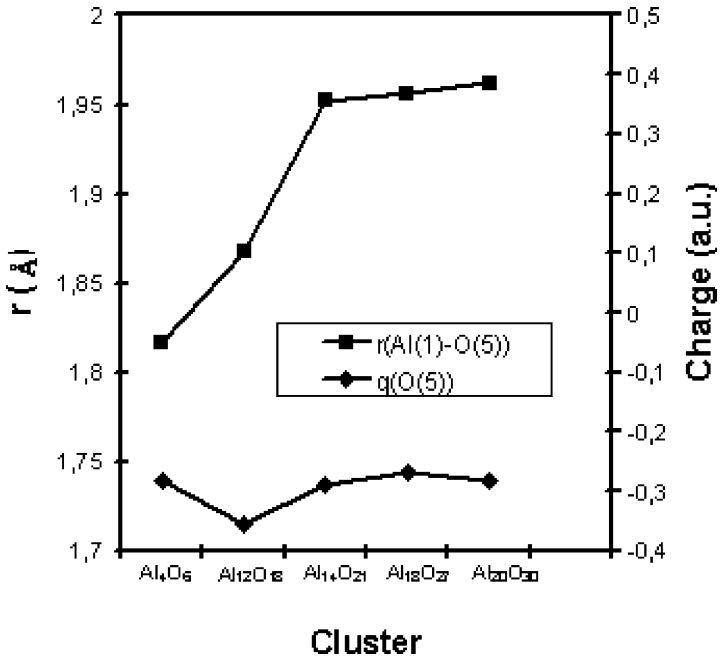

Fig. 4. Variation of equilibrium bond distance Al(1)–O(5) and charge on O(5) with the cluster size.

size of the cluster are shown in Fig. 4. The general trend is a convergence of these properties to constant values, as cluster size increases. In Fig. 5, variation bond strength (DBE) with atoms surrounding Al(1) Al(1)–O(X) bonds ($X = 2$–5) is presented. Results reveal a slower convergence in DBE, as the cluster size increases. In both figures, strong property changes are observed for small clusters, as expected. Therefore,

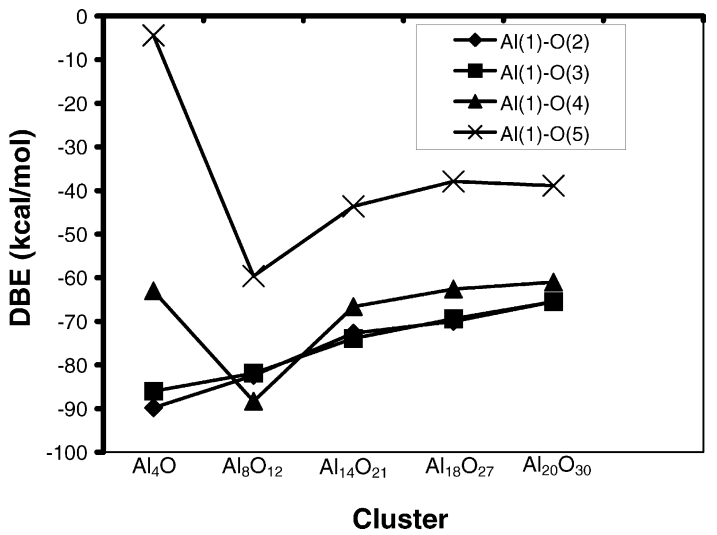

Fig. 5. Change of diatomic binding energies (DBE) for Al(1)–O(X) ($X = 1$–5) bonds with the cluster size.

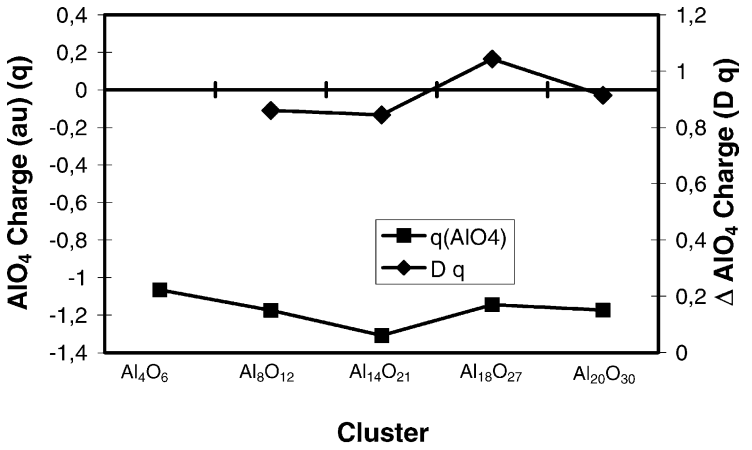

Fig. 6. Charge and charge change in the AlO_4 aggregate (adsorption site plus nearest-neighbors) as the cluster size increases.

one may conclude that for a fair representation of the adsorption site, a cluster size of reasonable size has to be considered. Notice that this requirement is necessary because charge transfer between regions A and BC is not allowed. In this case, the advantage of using parametric method is the possibility of handling in a practical way clusters of sufficient size. This electronic transference between atoms can be visualized by analyzing how the total charge density on Al(1) and its four oxygen ligand change with the cluster size.

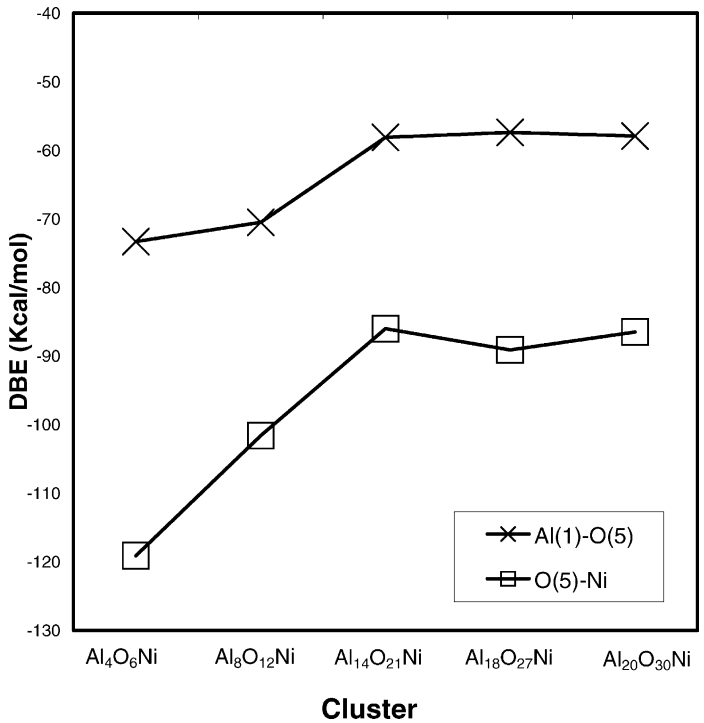

Fig. 7. Variation of Al(1)–O(5) and Ni–O(5) DBEs with the cluster size.

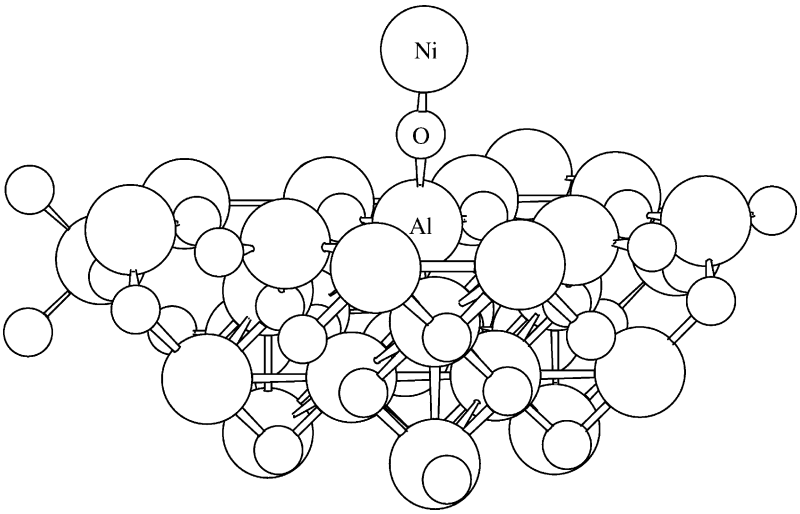

Fig. 8. $Al_{30}O_{45}Ni$ cluster used as reference for embedding.

The charge variation in the correspondent AlO_4 atoms from one size to other is presented in Fig. 6. As it can be seen, only for largest cluster charge changes tend to zero. Therefore, the best model for the support would be the $Al_{20}O_{30}$ cluster.

Because we are interested in the interaction of Ni dispersed on alumina, properties changes with the cluster size were also analyzed. The DBE changes for Al(1)–O(5) and Ni–O(5) are presented in Fig. 7, as it is going from Al_4O_6Ni to $Al_{20}O_{30}Ni$. The same trends are observed. Therefore, embedding of $Al_{20}O_{30}Ni$ was considered.

Parameters (for long- and short-range interaction functionals, see Eqs. (8) and (9), were obtained by adjusting them with respect to a larger cluster ($Al_{30}O_{45}Ni$, see Fig. 8) used as reference. The selected cluster ($Al_{20}O_{30}Ni$) was embedded into a set of point charges ($Al_{330}O_{643}$) that correspond to a cube in the (1 1 0) plane [11]. Before to evaluate embedding parameters, charges were balanced, considering the average value of charges obtained form a calculation of the largest cluster ($Al_{30}O_{45}$). The values of these point charges were: 0.605 for points charges representing Al atoms, and −0.424 for those corresponding to O atoms. Values of α parameters for core–core interactions were the same of those employed in molecular calculations. A reasonable adjustment was reached for λ_{XY} and ω_{XY} parameters (XY are the pairs Al–O, O–O, Ni–O, Ni–Al, and Al–Al) to reproduce the charge density on the O(5) atom of the largest cluster ($Al_{20}O_{30}$) (Table 3). Thus, the charge of O(5) in $Al_{20}O_{30}$ (−0.287) was partially reproduced by embedding (−0.274 a.u.).

In order to evaluate the effect of charges on an adsorption site formed by Ni clusters, a series of $Al_{20}O_{30}Ni_n$ ($n = 1$, 2, and 5) clusters were calculated with and without embedding. Values of Ni–O and Ni–Ni bond distances from the optimized cluster as well as DBEs are presented in Table 4. Values of embedded cluster are display in parentheses. The values of the optimal multiplicities are 3, 5, and 9 for $n = 1$,2, and 5, respectively.

Values of DBE show that Ni(1)–O(55) (see Fig. 9) is very strong as compare with Ni–Ni bonds. Therefore, it is expected that at very low coverage, Ni atoms prefer to bind oxygen atoms of the surface. The

Table 3
Embedding parameters

Parameter	Atom pair				
	Al–O	O–O	Al–Al	Ni–Al	Ni–O
ω	0.070	0.100	0.100	0.000	0.000
λ	0.100	0.069	0.130	0.070	0.035

Table 4
Bond distance, (values in parentheses in Å) and diatomic binding energies (DBEs in kcal/mol) for $Al_{20}O_{30}Ni_n$ ($n = 1,2$, and 5)[a]

Bond	System		
	$Al_{20}O_{30}Ni$ ($M = 3$)	$Al_{20}O_{30}Ni_2$ ($M = 5$)	$Al_{20}O_{30}Ni_5$ ($M = 9$)
O(55)–Ni(1)	−86.5	−89.5	−89.8
	−84.3*	−86.1*	−88.8*
	(1.806)	(1.800)	(1.808)
Ni(1)–Ni(2)	–	−42.6	−31.5
	–	−38.5*	−32.6*
	–	(2.252)	(2.469)
Ni(1)–Ni(3)	–	–	−9.0
	–	–	−9.1*
	–	–	(2.770)
Ni(2)–Ni(3)	–	–	−13.3
	–	–	−11.8*
	–	–	(2.438)
Ni(2)–Ni(4)	–	–	−23.2
	–	–	−23.0*
	–	–	(2.551)
Ni(3)–Ni(4)	–	–	−2.0
	–	–	−1.7*
	–	–	(2.802)
Ni(2)–Ni(5)	–	–	−11.6
	–	–	−9.9*
	–	–	(2.765)
Ni(4)–Ni(5)	–	–	−19.2
	–	–	−12.7*
	–	–	(2.263)

[a] Values with (*) correspond to embedded clusters. M values correspond to the optimal multiplicity.

addition of a second Ni atom (Ni(2)) produces a strong Ni–Ni bond with the characteristics of a diatomic molecule (−42.6 kcal/mol and 2.25 Å as compared with recent experimental values of binding energy and a bond length of −47.0 kcal/mol and 2.15 Å, respectively [51]). Clusters with $n = 3$ and 4 were found non-stable. In the $Al_{20}O_{30}Ni_5$ cluster (see Fig. 9), less saturated nickel atoms (Ni(3) and Ni(5) show the largest positive charge, as can be seen in Table 5. Experimentally have been found that alumina readily stabilizes ionic species, however, reduced Ni atoms have been also reported [52]. It is good to notice that Ni_n ($n = 2$–5) clusters were built up by adding one by one Ni atoms and then optimizing in each case. Therefore, it is probable that the obtained cluster geometry, as that of Fig. 9, corresponds to a local minimum, because global minimization of transition metal clusters are indeed troublesome [53].

Results also indicate that the effect of point charges (embedding case) is of decreasing Ni–Ni and Ni–O bonding interactions. The weakening of bond is about a 10%. In the case of atom charges, see Table 5, there is the trend to decrease charges on the O(5) atom. On the other hand, the positive charge tends to increase on Ni atoms except, in that Ni atom directly bonded to the O atom. Notice that these changes induced by the set of charges may be of importance in kinetics, charge distribution, and reactivity of the adsorption sites [54], mainly in charged transition states, as has been reported by others authors [55,56].

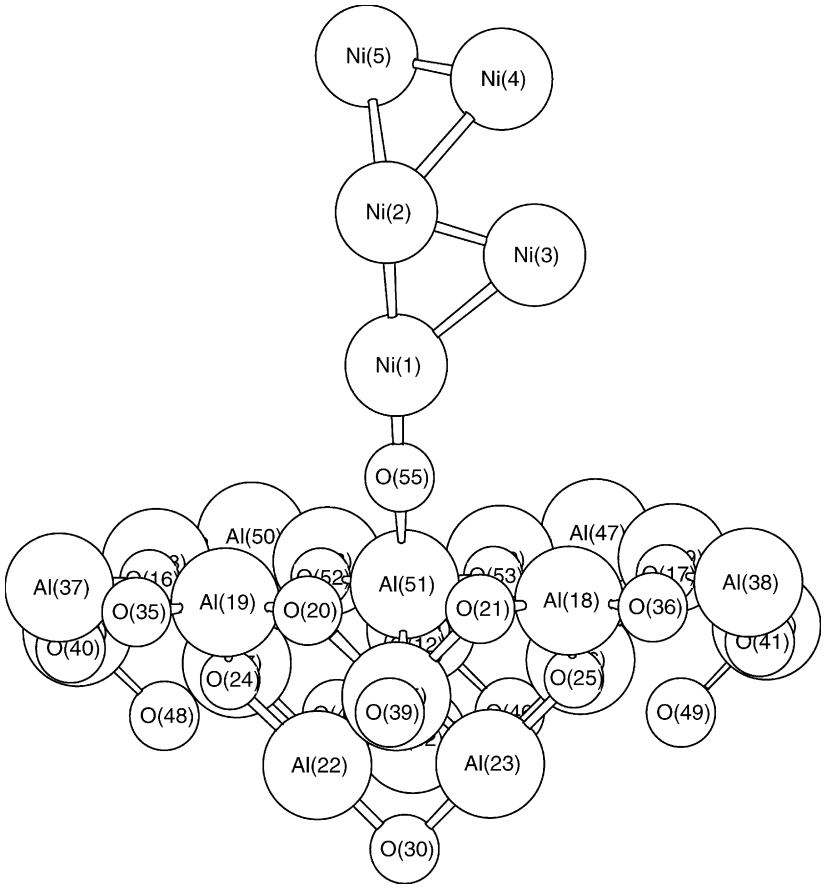

Fig. 9. $Al_{20}O_{30}Ni_5$ cluster.

Table 5
Charge on O(5) and Ni_n ($n = 1$–5) atoms with and without embedding[a]

System	Atom					
	O(55)	Ni(1)	Ni(2)	Ni(3)	Ni(4)	Ni(5)
$Al_{20}O_{30}Ni$	−0.262	0.077	–	–	–	–
$Al_{20}O_{30}Ni^*$	−0.265	0.077	–	–	–	–
$Al_{20}O_{30}Ni_2$	−0.230	−0.109	0.180	–	–	–
$Al_{20}O_{30}Ni_2{}^*$	−0.206	−0.134	0.227	–	–	–
$Al_{20}O_{30}Ni_5$	−0.265	0.062	0.080	0.351	0.151	0.245
$Al_{20}O_{30}Ni_5{}^*$	−0.249	0.019	0.087	0.360	0.174	0.283

[a] Values with (*) correspond to embedded clusters.

4. Conclusions and comments

(a) Parametric functionals can be employed to model short- and long-range interactions in embedding approximation used in parametrical methods. This approach improves the modeling of complex systems, such as, the effect of the support on surface active sites.

(b) Embedding approach for low symmetry systems, such as alumina, requires a minimum cluster size in order to reproduce, in a consistent way, properties of an extended system. Then, it is necessary to have an alumina cluster of enough size to avoid artifacts produced by an unsuitable selection of the catalyst model.
(c) For modeling one-center site, the minimum embedded cluster of alumina in alumina resulted to be an $Al_{20}O_{30}$ cluster whose property variations, such as, charge and DBEs tend to converge to constant values.
(d) The effect of the embedding on active site properties produces a decrease of Ni–O and Ni–Ni bond energies and an increase of the positive charge of the most exposed Ni atoms, a Ni_5 cluster.
(e) It is advisable to recommend a flexible code with the possibility of using a variable embedding, including a simple and practical parametrization methods. This will allow to reduce or to increase, in convenient cases, the size of the embedded model cluster.

Acknowledgements

This research has been supported by CONICIT under contracts G-9700667. FMP thank Universidad Nacional de Colombia, Facultad de Ciencias for allowing the use of workstations. We also thank referees for helpful suggestions.

References

[1] B. Kirtman, C.P. DeMelo, J. Chem. Phys. 79 (1981) 4592.
[2] M. Matos, B. Kirtman, C.P. DeMelo, J. Chem. Phys. 88 (1988) 1019.
[3] M.S. Daw, M.I. Baskes, Phys. Rev. B 29 (1984) 6443.
[4] S.M. Foiles, M.I. Baskes, M.S. Daw, Phys. Rev. B 33 (1986) 7983.
[5] J.L. Whitten, T.A. Pakkanen, Phys. Rev. B 21 (1980) 4357.
[6] H. Yang, J.L. Whitten, J. Phys. Chem. 100 (1996) 5090.
[7] Z. Barandarián, L. Seijo, J. Chem. Phys. 89 (1988) 5739.
[8] J.L. Pascual, L. Seijo, J. Chem. Phys. 102 (1995) 5368.
[9] J.A. Mejías, J. Fernandez-Sanz, J. Chem. Phys. 102 (1995) 327.
[10] J.A. Mejías, J. Fernandez-Sanz, J. Chem. Phys. 102 (1995) 850.
[11] J. Fernandez-Sanz, H. Rabaa, F.M. Poveda, A.M. Márquez, C.J. Calzado, Int. J. Quantum Chem. 70 (1998) 359.
[12] H.A. Duarte, D.R. Salahub, J. Chem. Phys. 108 (1998) 743.
[13] N. Govind, Y.A. Wang, A.J.R. da Silva, E.A. Carter, Chem. Phys. Lett. 295 (1998) 129.
[14] T. Zhu, W. Pan, W. Yang, Phys. Rev. B 53 (1996) 12713.
[15] H. Zheng, Phys. Lett. A 226 (1997) 223.
[16] U. Gutdeutsch, U. Birkenheuer, N. Rösch, J. Chem. Phys. 109 (1998) 2056.
[17] A.L. Shluger, J.D. Gale, Phys. Rev. B 54 (1996) 962.
[18] P.V. Sushko, A.L. Shluger, C.R.A. Catlow, Surf. Sci. 450 (2000) 153.
[19] S.A. French, A.A. Sokol, S.T. Bromley, C.R.A. Catlow, S.C. Rogers, F. King, P. Sherwood, Angew Chem. Int. Ed. 40 (2001) 4437.
[20] C. Pisani, R. Dovesi, R. Nada, L.N. Kantorovich, J. Chem. Phys. 92 (1990) 7448.
[21] C. Pisani, U. Birkenheuer, Int. J. Quantum Chem. S29 (1995) 221.
[22] M.I. Trioni, G.P. Brivio, S. Crampin, J.E. Inglesfield, Phys. Rev. 53 (1996) 8052, and references therein.
[23] A. Shukla, M. Dolg, H. Stoll, P. Fulde, Chem. Phys. Lett. 262 (1996) 213.
[24] H. Donnerberg, R.H. Bartram, J. Phys. Condens. Mat. 8 (1996) 1687.
[25] J.D. Head, S.J. Silva, J. Chem. Phys. 104 (1996) 3244.
[26] X. Xu, H. Nakatsuji, M. Ehara, X. Lü, N.Q. Wang, Q.E. Zhang, Chem. Phys. Lett. 292 (1998) 282.
[27] T. Bredow, G. Geudtner, K. Jug, J. Chem. Phys. 105 (1996) 6395.
[28] D. Nanda, K. Jug, Theor. Chim. Acta 57 (1980) 95.
[29] S. Katsuki, S. Huzinaga, Chem. Phys. Lett. 152 (1988) 203.
[30] S. Huzinaga, J. Mol. Struct., Theochem. 234 (1991) 51.
[31] J.A. Pople, D.L. Beveridge, Approximate Molecular Orbital Theory, McGraw-Hill, New York, 1970, pp. 60, 76.
[32] K. Jug, Theor. Chim. Acta 14 (1969) 91.
[33] M. Romero, J.R. Primera, M. Sánchez, A. Sierraalta, S. Brassesco, J. Bravo, F. Ruette, Folia Chim. Theor. Latina 23 (1995) 45.
[34] J.R. Primera, M. Romero, M. Sánchez, A. Sierralta, F. Ruette, J. Mol. Struct., Theochem. 469 (1999) 177.
[35] K. Ohno, Theor. Chim. Acta 2 (1964) 2191.
[36] G. Klopman, J. Am. Chem. Soc. 86 (1964) 4550.
[37] G. Blyholder, J. Head, F. Ruette, Theor. Chim. Acta 60 (1982) 429.
[38] M. Romero, M. Sánchez, A. Sierraalta, L. Rincón, F. Ruette, J. Chem. Infor. Comp. Sci. 39 (1999) 543.
[39] F. Ruette, M. Sánchez, G. Martorell, C. González, R. Añez, A. Sierraalta, L. Rincón, C. Mendoza, submitted for publication.
[40] C.E. Moore, Atomic Energy Levels, National Standard Reference Data Series, Vol. 1, Nat. Bur. Stand., Washington, 1971.
[41] C. González, Un método paralelo de recocido simulado usando MonteCarlo, in: L.J. Alvarez (Ed.), Métodos Computacionales en la Catálisis, UNAM, CYTED, México, in press.
[42] F. Ruette, G. Blyholder, J. Head, J. Chem. Phys. 80 (1984) 2042.
[43] B. Rosen, Spectroscopic Data Relative to Diatomic Molecule, Pergamon Press, Oxford, 1970.

[44] K.P. Huber, G. Hersberg, Molecular Spectra and Molecular Structure, Vol. 4, Van Nostrand Reinhold, New York, 1979.
[45] J.M. Behm, C.A. Arrington, M.D. Morse, J. Chem. Phys. 99 (1993) 6409.
[46] J.F. Harrison, Chem. Rev. 100 (2000) 679.
[47] H. Kawakami, S. Yoshida, J. Chem. Soc., Faraday Trans. 81 (1985) 1117.
[48] M.B. Fleisher, L.O. Golender, N.V. Shimanskaya, J. Chem. Soc., Faraday Trans. 87 (1991) 745.
[49] H. Tachikawa, T. Tsuchida, J. Mol. Catal., A Chem. 96 (1995) 277.
[50] A. Zecchina, E. Escalona Platero, C. Otero Areán, J. Catal. 107 (1987) 244.
[51] J.C. Pinegar, J.D. Langenberg, C.A. Arrington, E.M. Spain, M.D. Morse, J. Chem. Phys. 102 (1995) 666.
[52] J.B. Peri, J. Catal. 86 (1984) 84.
[53] F. Ruette, C. González, Chem. Phys. Lett., in press.
[54] L. Leherte, J.M. Andre, D.P. Vercauteren, E.G. Derouane, J. Mol. Catal. 54 (1989) 426.
[55] E.H. Teunissen, A.P.J. Hansen, R.A. van Santen, J. Chem. Phys. 101 (1994) 5865.
[56] S.P. Greatbanks, I.H. Hillier, P. Sherwood, J. Comp. Chem. 18 (1997) 562.